

Origin of Metastable Knots in Single Flexible Chains

Liang Dai,¹ C. Benjamin Renner,² and Patrick S. Doyle^{1,2,*}

¹BioSystems and Micromechanics IRG, Singapore-MIT Alliance for Research and Technology Centre, Singapore 117543, Singapore

²Department of Chemical Engineering, Massachusetts Institute of Technology (MIT), Cambridge, Massachusetts 02139, USA

(Received 28 October 2014; published 22 January 2015)

Recent theoretical progress has explained the physics of knotting of semiflexible polymers, yet knotting of flexible polymers is relatively unexplored. We herein develop a new theory for the size distribution of knots on a flexible polymer and the existence of metastable knots. We show the free energy of a flexible molecule in a tube can be mapped to quantitatively reproduce the free energy distribution of a knot on a flexible chain. The size distribution of knots on flexible chains is expected to be universal and might be observed at a macroscopic scale, such as a string of hard balls.

DOI: 10.1103/PhysRevLett.114.037801

PACS numbers: 61.41.+e, 02.10.Kn, 87.10.Rt, 87.15.-v

Long polymer molecules can find themselves in knotted conformations, akin to those seen in jumbled strings [1] or agitated chains [2–4], and these knots become increasingly likely as the length of the polymer is increased [5]. Knotted conformations are frequently found in polymers in poor solvents [6] or confined within small volumes, such as a viral capsid [7,8], and a number of knotted protein conformations have been discovered [9–11]. To study the properties of knots on polymers more closely, knots have been tied on actin filaments [12] and DNA molecules [13] with optical tweezers, and knots have been generated on DNA in microfluidic devices through collisions with defects [14] or the application of electric fields [15]. Simple knots can influence dynamic polymer processes such as breaking a strand [16], rheological response [17], translocation of a protein [18,19] or DNA [20] through a pore, or the ejection of DNA from a viral capsid [21]. The specific topology of a knot can also alter rates of ejection from the viral capsid [22] and untying in electric fields [23,24]. Composite knots have been shown to exhibit complex dynamics [25]. Recently, researchers have shown how to generate knots of selected topologies in polymers via chemical synthesis pathways [26,27] and self-assembly [28].

These developments have motivated fundamental study of knots on polymers. The knotting probability and the size distribution of knots have been investigated for chains under various conditions [29–35]. An intriguing finding from simulations is that the cores of knots often localize to small portions of semiflexible [36] or flexible chain [6,37–40] [Fig. 1(a)]. Grosberg and Rabin posited a theory that predicts a metastable knot size for thin semiflexible polymers, such as double-stranded DNA [41]. The Grosberg-Rabin (GR) theory considers the bending and confining energies within the knot, which tend to swell and shrink the knot, respectively, leading to a metastable size. We extended the GR theory to incorporate the effect of a finite chain width and demonstrated quantitative agreement between these theories and simulation results [36]. These

theories, however, cannot address knotting in flexible chains, such as single-stranded DNA and most common synthetic polymers, yet recent simulations observed a metastable knot size in these flexible molecules [40].

In this Letter, we present a new theory that predicts a metastable knot size for *flexible* polymers. We show results of simulations of trefoil knots in long, flexible polymer molecules exhibit a metastable knot size. We develop a theory that considers a flexible knot to be effectively confined in a virtual tube, and we perform simulations to understand the free energy of confinement of flexible chains in tubes. Finally, we show that the simulations of flexible chains in tubes can be directly mapped to the free energies of knots by the choice of two reasonable fitting parameters.

We performed Monte Carlo simulation of flexible chains and analyzed conformations of the trefoil knot. In our simulations, the flexible chain is modeled as a string of

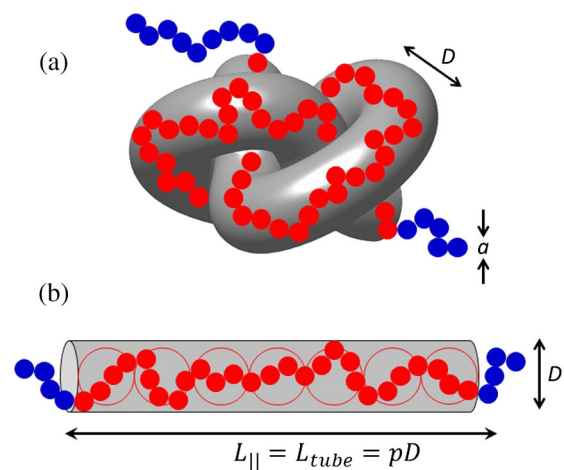


FIG. 1 (color online). (a) A trefoil knot in a flexible chain. The monomers in the knotted region (red) are confined in a virtual tube (gray). (b) A flexible chain confined in a tube. The open circles correspond to blobs of size $D_{\text{eff}} = D - a$.

hardcore beads, each with diameter a . In each Monte Carlo cycle, either a crankshaft or reptation move is performed, described in Ref. [42]. The algorithm of calculating knot sizes has been presented in our previous publication [36] and is briefly recapitulated here. We used the minimally interfering closure scheme [43] to generate closed configurations of the chain, and we calculated the Alexander polynomial $\Delta(t)$ [44] of this closed loop. We identified the knotted subregion by successively cutting segments from ends of the chain, generating a new closure, and recalculating $\Delta(t)$ until detecting a change in $\Delta(t)$. The knot size L_{knot} is defined as the contour length inside the knotted subregion.

The probability of forming a trefoil knot of a certain size L_{knot} is shown in Fig. 2(a) for simulations of 2000 and 1000 monomers. The probability $f_{\text{knot}}(x)$ is normalized such that $\int_0^{+\infty} f_{\text{knot}}(x)dx = f_{\text{total}}$, where $x = L_{\text{knot}}/a$ and $f_{\text{total}} \approx 0.00226$ or 0.00094 is the total probability of a trefoil knot for simulations of 2000 or 1000 monomers, respectively. In agreement with a previous study [40], f_{knot} is maximized at a critical knot size $L_{\text{knot}}^* = (140 \pm 20)a$, corresponding to a metastable knot. The values of f_{knot} for $L = 1000$ are approximately half that of $L = 2000$ over the range $L_{\text{knot}} \leq 700$, which suggests the metastable knots are insensitive to the contour length; a similar result was obtained in a previous study [40]. The values of f_{knot} are converted to the free energy by

$$F_{\text{knot}} = -\log(f_{\text{knot}}). \quad (1)$$

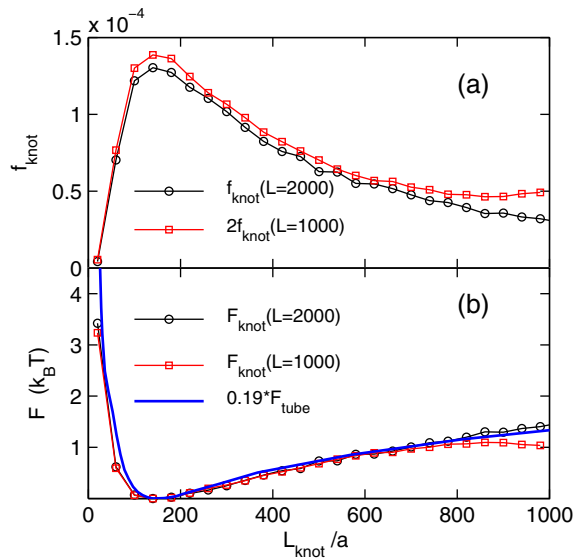


FIG. 2 (color online). (a) Probability of forming a trefoil knot of a certain size for chains of $L = 2000$ and $L = 1000$ monomers. The probabilities for $L = 1000$ are scaled by a factor of 2. (b) Free energies as a function of knot size from computer simulations (circles). The blue line is the rescaled free energy of a flexible polymer in a straight tube, using Eqs. (7), (8), and data in Fig. 3(c).

In Eq. (1) and throughout this Letter, all free energies, F_i , are made dimensionless by $k_B T$. Figure 2(b) shows the free energy as a function of L_{knot} after shifting the minimum to zero. The trefoil knot attains a minimum free energy at $L_{\text{knot}}^* \approx 140a$. A well depth of $\sim 1k_B T$ spans from $50 < L_{\text{knot}}/a < 700$, diverging sharply for smaller knots and rising gradually for larger knots.

We will now focus on the physics governing the distribution of knot sizes on flexible polymer molecules. We show that using a renormalized free energy of a flexible chain confined in a hard tube, the distribution of sizes of trefoil knots can be quantitatively captured, as indicated by the agreement between the blue line (free energy of flexible chains in hard tubes) and black and red circles (free energies of knots) in Fig. 2(b). For the remainder of this Letter, we will explain the physics behind the confinement of a flexible chain in a tube and how this leads to a metastable knot on a flexible chain.

For semiflexible chains, Grosberg and Rabin [41] envisioned the monomers in the knotted region to be confined in a virtual tube, depicted in Fig. 1(b). The self-confinement free energy in knots F_{knot} can be mapped to the confinement free energy of a chain confined in a straight tube F_{tube} , a more tractable problem. The virtual tube can be imaged as the state of a maximally inflated knot, and so the characteristic ratio

$$p \equiv L_{\text{tube}}/D \quad (2)$$

only depends on the topology of the knot [45]. Here, D and L_{tube} denote the diameter and length of the tube, respectively. This definition allows the problem of minimizing F_{knot} with respect to the knot size L_{knot} to be solved via the ansatz of minimizing F_{tube} with respect to D under the condition $L_{\text{tube}} = pD$.

We turn to the chains confined in straight tubes [Fig. 1(b)]. The confinement free energy can be written as

$$F_{\text{tube}} = F_m N_m, \quad (3)$$

where F_m is the confinement free energy per monomer, and $N_m = L_{\text{knot}}/a$ is the number of confined monomers. Using the definition of the relative extension r of the chain in a tube,

$$r \equiv L_{\text{tube}}/(N_m a), \quad (4)$$

the number of confined monomers can be written as $N_m = pD/(ra)$. Recall that L_{tube} in Eq. (4) equals the extension of the confined chain. In our theory and simulations, the effective tube diameter

$$D_{\text{eff}} \equiv D - a, \quad (5)$$

is more relevant than D because the centers of monomers are confined in a tube of diameter D_{eff} rather than D . Using Eq. (5), we modify Eq. (3) to

$$F_{\text{tube}} = pF_m/r \times (D_{\text{eff}}/a + 1). \quad (6)$$

The above equation indicates that F_{tube}/p only depends on D_{eff} because F_m and r depend solely on D_{eff}/a . To numerically obtain $F_m(D_{\text{eff}})$ and $r(D_{\text{eff}})$, we performed additional simulations of confined flexible chains containing 1000 monomers. The relative extension $r(D_{\text{eff}})$ was obtained using typical Monte Carlo simulations as described above. The confinement free energies F_m were obtained by the Pruned-Enriched Rosenbluth Method (PERM) simulations [46]. The details of the PERM algorithm were presented in our previous publication [47].

Figures 3(a) and 3(b) show F_m and r as a function of D_{eff} , calculated from simulation results. From these results, Eq. (6) was used to calculate F_{tube}/p as a function of D_{eff} , shown in Fig. 3(c). In qualitative agreement with the observed metastable knot sizes in Fig. 2, a local minimum exists at $D_{\text{eff}}^* = 3.0a$. The excellent agreement between theory and simulation shown in Fig. 2(b) was achieved by a mapping of the results in Fig. 3, described as follows. The relationship between D_{eff} and L_{knot} is

$$L_{\text{knot}} = p(D_{\text{eff}} + a)/r. \quad (7)$$

A value of $p = 17.9$ was used in order to match the minimum location $D_{\text{eff}}^* = 3.0a$ in Fig. 3(c) and the minimum location $L_{\text{knot}}^* = 140a$ in Fig. 2(b). This value of p is close to a similarly fit value of $p = 16$ for the semiflexible chains [36], and the ideal value 12.4 for the maximally inflated trefoil knot [45]. We rescaled the free energy of confinement by a factor of

$$\alpha = F_{\text{knot}}/F_{\text{tube}}. \quad (8)$$

The fitted value of $\alpha = 0.19 < 1$ corrects for the fact that the virtual tube of the knot has soft (rather than hard) walls. With these two parameters, the numerical values from simulations of a flexible chain confined to a hard tube are mapped onto the free energy of trefoil (3_1) knots (blue curve, Fig. 2). Similar results for 4_1 knots are shown in the Supplemental Material [48]. These results strongly suggest that the physics of the knotted region of a flexible chain are that of self-confinement, similar to the physics in semiflexible chains [36].

While the above analysis paints a compelling picture, *why* the local minimum of F_{tube} with respect to D_{eff} exists is not obvious and merits further discussion. We write F_{tube} as

$$F_{\text{tube}} = N_{\text{blob}}F_{\text{blob}}, \quad (9)$$

where F_{blob} is the confinement free energy within a blob of size D_{eff} [Fig. 1(b)]. Note that the ‘‘blob’’ in this Letter simply corresponds to the subchain within a sphere of diameter D_{eff} . Considering that the tube length is pD and the extension of each blob is D_{eff} , the number of blobs is

$$N_{\text{blob}} = p(1 + a/D_{\text{eff}}). \quad (10)$$

It is easy to see that $N_{\text{blob}} \rightarrow p$ as $D_{\text{eff}} \rightarrow \infty$, and $N_{\text{blob}} \rightarrow \infty$ as $D_{\text{eff}} \rightarrow 0$. Figure 3(d) shows F_{blob} versus D_{eff} calculated from F_m and r in Figs. 3(a) and 3(b) using

$$F_{\text{blob}} = F_m D_{\text{eff}}/(ra). \quad (11)$$

In weak confinement, $D_{\text{eff}} \gg a$, the classic blob model [49,50] predicts the confinement free energy per blob is independent of blob size:

$$F_{\text{blob}} = c_1, \quad (12)$$

where c_1 is determined to be $5.0k_B T$ in Fig. 3(d).

In strong confinement, $D_{\text{eff}} \ll a$, we can derive the expressions of F_m and r as follows. In the absence of confinement and excluded volume (EV) interactions, the allowed region for the vector connecting two monomers is a sphere with surface area $4\pi a^2$. Considering the EV of three adjacent monomers, the allowed space becomes $3\pi a^2$. In a tube, the allowed region for the vector connecting two monomers corresponds to the cross section of the tube, and the area is $\pi(D_{\text{eff}}/2)^2$. The entropy loss per monomer is

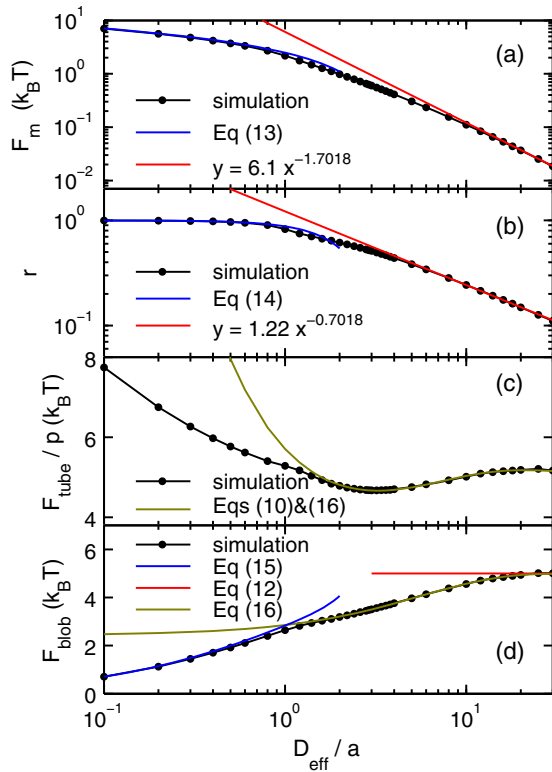


FIG. 3 (color online). (a) The confinement free energy per monomer as a function of the effective tube diameter. (b) The relative extension as a function of the effective tube diameter. (c) The total confinement free energy divided by p as a function of the effective tube diameter. (d) The confinement free energy per blob as a function of the effective tube diameter. The red lines are based on the scalings predicted by the blob model [49,50] and the Flory exponent $\nu = 0.5876$ [51]. The prefactors are the best fit values.

$$F_m = -\log[D_{\text{eff}}^2/(12a^2)]. \quad (13)$$

The average angle between the tube axis and the vector connecting two monomers is $\text{asin}[D_{\text{eff}}/(2a)] \approx D_{\text{eff}}/(2a)$. Then, the average extension of each monomer along the tube axis is

$$r = \cos[D_{\text{eff}}/(2a)]. \quad (14)$$

Using Eqs. (13) and (14), the confinement free energy per blob in strong confinement is

$$F_{\text{blob}} = -(D_{\text{eff}}/a) \log[D_{\text{eff}}^2/(12a^2)] / \cos[D_{\text{eff}}/(2a)]. \quad (15)$$

Equation (15) indicates that $F_{\text{blob}} = 0$ when $D_{\text{eff}}/a = 0$, agreeing with the simulation results in Fig. 3(d).

We have obtained agreement between theory and simulations for F_{blob} in weak and strong confinements, which are observed to be applicable for $D_{\text{eff}} \geq 20a$ and $D_{\text{eff}} \leq 0.2a$, respectively. The critical tube diameter, $D_{\text{eff}}^* \approx 3.0a$, which corresponds to the metastable knot size, is located in the transition regime between these two extreme cases. At the critical tube diameter, $r = 0.51$ and $F_m = 0.60k_B T$. We propose an empirical expression for F_{blob} in the transition regime

$$F_{\text{blob}} = 5.0 - 2.57 \exp(-0.18D_{\text{eff}}/a), \quad (16)$$

which agrees with the simulation results for $D_{\text{eff}} \geq 2a$ [Fig. 3(d)]. By using Eqs. (16) and (10) with Eq. (9), we are able to reproduce the free energy landscape for $D_{\text{eff}} \geq 2a$, which covers the local minimum.

In order to understand why F_{blob} decreases monotonically as the blob size decreases in the transition regime, we analyzed the orientation correlation $\langle \mathbf{u}_i \cdot \mathbf{u}_j \rangle$ as a function of the separation $s = |j - i|$ between pairs of bond unit vectors \mathbf{u}_i and \mathbf{u}_j in bulk, shown in Fig. 4. Here, the brackets indicate averaging over all i, j , and molecules. The positive correlation indicates the relative orientation between two adjacent blobs (subchains) is not completely random in bulk. This correlation is due to EV interactions which disfavor backfolding of the chain. Hence, the positive correlation reduces the free energy cost of aligning

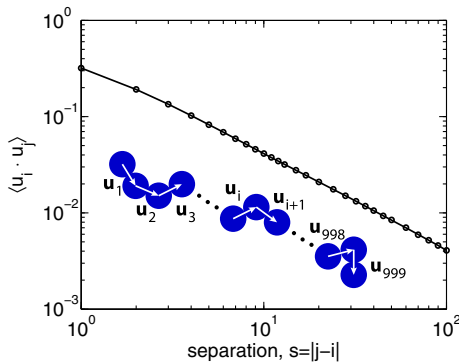


FIG. 4 (color online). Orientation correlation as a function of monomer separation for a flexible chain in bulk ($L = 1000$).

blobs, reducing F_{blob} . Such a correlation explains why F_{blob} is smaller than the asymptotic value c_1 in the transition regime. Note that for the critical tube diameter $D_{\text{eff}} = 3.0a$, the number of monomers in the blob is approximately 6. The correlation for $s = 6$ in bulk is 0.07.

With the theory for knot sizes in flexible chains now established, we will compare it to the GR theory for semiflexible chains. For semiflexible chains, the metastable knot size is set by the bending energy, which scales as $F_{\text{bend}} \sim L_{\text{knot}}^{-1}$, and the confinement free energy, which scales as $F_{\text{confine}} \sim L_{\text{knot}}^{1/3}$. It is apparent that the competition between these terms can lead to a minimum of free energy. Note that the GR theory for semiflexible chains predicts shrinking forces exist *only* for sufficiently tight knots but not for looser knots in semiflexible chains [36] or knots in flexible chains. For flexible chains, there is no bending energy F_{bend} . In this case, the minimum of F_{confine} cannot be intuited from its asymptotic behavior: (i) $F_{\text{confine}} \rightarrow \infty$ as $L_{\text{knot}} \rightarrow 0$, (ii) $F_{\text{confine}} \rightarrow pc_1$ as $L_{\text{knot}} \rightarrow \infty$. A minimum of F_{confine} , however, is revealed in the simulation results in the transition regime. If we examine what happens when EV interactions are ignored, the confinement free energies F_{confine} of flexible and semiflexible chains become similar. For flexible chains in the absence of EV, we have $D_{\text{eff}} = D$, and $F_{\text{confine}} = pF_{\text{blob}}$ should decrease towards zero for $L_{\text{knot}} \rightarrow 0$, as seen in semiflexible chains. This effect serves to tighten a knot as much as possible. For simulations of trefoil knots on fully flexible chains without EV, Katrich *et al.* [37] found a most probable size of 7 segments, and our simulations (see Supplemental Material [48]) find a value of 6 segments. Both values are remarkably close to 5 segments, the minimum number required to form a trefoil knot. The larger knots observed in simulations may arise from the high curvature in the virtual tube (versus the straight tube in theory).

Our results imply that once a knot is formed on a long flexible chain, the knot will diffuse along the chain with its size fluctuating around L_{knot}^* for a certain period before escaping the potential well or it is untied at the chain ends (see Supplemental Material [48]). This behavior has been observed in previous simulations [40]. More broadly, a knot can be considered as a number of self-entanglements of a chain, sharing similarities with entanglements in multichain systems. The effective potentials induced by the virtual tubes of knots are similar to those induced by entanglements in multichain systems [36,52]. However, the interchain entanglements are more abundant than self-entanglements in entangled polymer melts [53,54].

We have developed a simple theory to explain the origins of metastable knots on flexible polymer molecules. These knots localize due to two competing effects: shrinking to reduce the number of monomers in the confined, knotted region and swelling to reduce the effective confinement free energy for each of these monomers. For trefoil knots, the metastable state contains 140 ± 20 monomers, and these monomers can be imaged to be confined in a virtual tube

of diameter $4.0a$ and length $71.7a$. Looking forward, the equilibrium distribution of knot size around the metastable knot size is expected to be universal and may be also applied to agitated macroscopic strings [1–4]. However, experiments of knots on macroscopic chains are typically on planes [2,4], while our simulation and theory are for 3D chains.

This research was supported by the National Research Foundation Singapore through the Singapore MIT Alliance for Research and Technology's research programme in BioSystems and Micromechanics and the National Science Foundation (Grant No. 1335938).

*pdoyle@mit.edu

- [1] D. M. Raymer and D. E. Smith, *Proc. Natl. Acad. Sci. U.S.A.* **104**, 16432 (2007).
- [2] E. Ben-Naim, Z. A. Daya, P. Vorobieff, and R. E. Ecke, *Phys. Rev. Lett.* **86**, 1414 (2001).
- [3] A. Belmonte, M. J. Shelley, S. T. Eldakar, and C. H. Wiggins, *Phys. Rev. Lett.* **87**, 114301 (2001).
- [4] J. Hickford, R. Jones, S. C. du Pont, and J. Eggers, *Phys. Rev. E* **74**, 052101 (2006).
- [5] D. W. Sumners and S. G. Whittington, *J. Phys. A* **21**, 1689 (1988).
- [6] P. Virnau, Y. Kantor, and M. Kardar, *J. Am. Chem. Soc.* **127**, 15102 (2005).
- [7] J. Arsuaga, M. Vázquez, S. Trigueros, D. W. Sumners, and J. Roca, *Proc. Natl. Acad. Sci. U.S.A.* **99**, 5373 (2002).
- [8] J. Arsuaga, M. Vazquez, P. McGuirk, S. Trigueros, D. W. Sumners, and J. Roca, *Proc. Natl. Acad. Sci. U.S.A.* **102**, 9165 (2005).
- [9] W. R. Taylor and K. Lin, *Nature (London)* **421**, 25 (2003).
- [10] P. Virnau, L. A. Mirny, and M. Kardar, *PLoS Comput. Biol.* **2**, e122 (2006).
- [11] G. Kolesov, P. Virnau, M. Kardar, and L. A. Mirny, *Nucleic Acids Res.* **35**, W425 (2007).
- [12] Y. Arai, R. Yasuda, K.-i. Akashi, Y. Harada, H. Miyata, K. Kinoshita, and H. Itoh, *Nature (London)* **399**, 446 (1999).
- [13] X. R. Bao, H. J. Lee, and S. R. Quake, *Phys. Rev. Lett.* **91**, 265506 (2003).
- [14] R. Metzler, W. Reisner, R. Riehn, R. Austin, J. Tegenfeldt, and I. M. Sokolov, *Europhys. Lett.* **76**, 696 (2006).
- [15] J. Tang, N. Du, and P. S. Doyle, *Proc. Natl. Acad. Sci. U.S.A.* **108**, 16153 (2011).
- [16] A. M. Saitta, P. D. Soper, E. Wasserman, and M. L. Klein, *Nature (London)* **399**, 46 (1999).
- [17] D. Kivotides, S. L. Wilkin, and T. G. Theofanous, *Phys. Rev. E* **80**, 041808 (2009).
- [18] L. Huang and D. E. Makarov, *J. Chem. Phys.* **129**, 121107 (2008).
- [19] P. Szymczak, *Eur. Phys. J. Spec. Top.* **223**, 1805 (2014).
- [20] A. Rosa, M. Di Ventra, and C. Micheletti, *Phys. Rev. Lett.* **109**, 118301 (2012).
- [21] R. Matthews, A. A. Louis, and J. M. Yeomans, *Phys. Rev. Lett.* **102**, 088101 (2009).
- [22] D. Marenduzzo, C. Micheletti, E. Orlandini, and D. W. Sumners, *Proc. Natl. Acad. Sci. U.S.A.* **110**, 20081 (2013).
- [23] M. Di Stefano, L. Tubiana, M. Di Ventra, and C. Micheletti, *Soft Matter* **10**, 6491 (2014).
- [24] C. B. Renner and P. S. Doyle, *ACS Macro Lett.* **3**, 963 (2014).
- [25] B. Trefz, J. Siebert, and P. Virnau, *Proc. Natl. Acad. Sci. U.S.A.* **111**, 7948 (2014).
- [26] J.-F. Ayme, J. E. Beves, D. A. Leigh, R. T. McBurney, K. Rissanen, and D. Schultz, *Nat. Chem.* **4**, 15 (2012).
- [27] N. Ponnuswamy, F. B. Cougnon, J. M. Clough, G. D. Pantoş, and J. K. Sanders, *Science* **338**, 783 (2012).
- [28] I. Coluzza, P. D. J. van Oostrum, B. Capone, E. Reimhult, and C. Dellago, *Phys. Rev. Lett.* **110**, 075501 (2013).
- [29] R. Metzler, A. Hanke, P. G. Dommersnes, Y. Kantor, and M. Kardar, *Phys. Rev. Lett.* **88**, 188101 (2002).
- [30] E. Ercolini, F. Valle, J. Adamcik, G. Witz, R. Metzler, P. De Los Rios, J. Roca, and G. Dietler, *Phys. Rev. Lett.* **98**, 058102 (2007).
- [31] R. Matthews, A. A. Louis, and C. N. Likos, *ACS Macro Lett.* **1**, 1352 (2012).
- [32] P. Poier, C. N. Likos, and R. Matthews, *Macromolecules* **47**, 3394 (2014).
- [33] C. Micheletti and E. Orlandini, *Soft Matter* **8**, 10959 (2012).
- [34] E. Orlandini, M. Tesi, and S. Whittington, *J. Phys. A* **38**, L795 (2005).
- [35] L. Dai, J. R. van der Maarel, and P. S. Doyle, *ACS Macro Lett.* **1**, 732 (2012).
- [36] L. Dai, C. B. Renner, and P. S. Doyle, *Macromolecules* **47**, 6135 (2014).
- [37] V. Katritch, W. K. Olson, A. Vologodskii, J. Dubochet, and A. Stasiak, *Phys. Rev. E* **61**, 5545 (2000).
- [38] E. Guitter and E. Orlandini, *J. Phys. A* **32**, 1359 (1999).
- [39] C. H. Nakajima and T. Sakaue, *Soft Matter* **9**, 3140 (2013).
- [40] L. Tubiana, A. Rosa, F. Fragiaco, and C. Micheletti, *Macromolecules* **46**, 3669 (2013).
- [41] A. Y. Grosberg and Y. Rabin, *Phys. Rev. Lett.* **99**, 217801 (2007).
- [42] L. Dai, J. J. Jones, J. R. van der Maarel, and P. S. Doyle, *Soft Matter* **8**, 2972 (2012).
- [43] L. Tubiana, E. Orlandini, and C. Micheletti, *Prog. Theor. Phys. Suppl.* **191**, 192 (2011).
- [44] M. Frank-Kamenetskii and A. Vologodskii, *Sov. Phys. Usp.* **24**, 679 (1981).
- [45] P. Pierański, S. Przybył, and A. Stasiak, *Eur. Phys. J. E* **6**, 123 (2001).
- [46] P. Grassberger, *Phys. Rev. E* **56**, 3682 (1997).
- [47] L. Dai, J. van der Maarel, and P. S. Doyle, *Macromolecules* **47**, 2445 (2014).
- [48] See Supplemental Material at <http://link.aps.org/supplemental/10.1103/PhysRevLett.114.037801> for simulation results of 4_1 knots and ideal chains; discussion about knot dynamics.
- [49] P. G. De Gennes, *Scaling Concepts in Polymer Physics* (Cornell Univ. Press, Ithaca, NY, 1979).
- [50] S. Jun, D. Thirumalai, and B.-Y. Ha, *Phys. Rev. Lett.* **101**, 138101 (2008).
- [51] N. Clisby, *Phys. Rev. Lett.* **104**, 055702 (2010).
- [52] Q. Zhou and R. G. Larson, *Macromolecules* **39**, 6737 (2006).
- [53] E. Panagiotou, M. Kröger, and K. C. Millett, *Phys. Rev. E* **88**, 062604 (2013).
- [54] S. K. Sukumaran, G. S. Grest, K. Kremer, and R. Everaers, *J. Polym. Sci., Part B: Polym. Phys.* **43**, 917 (2005).